POLITECNICO DI TORINO
Repository ISTITUZIONALE

Effect of Engine Start and Clutch Slip Losses on the Energy Management Problem of a Hybrid DCT Powertrain

(Article begins on next page)

19 April 2024

EFFECT OF ENGINE START AND CLUTCH SLIP LOSSES ON THE ENERGY MANAGEMENT PROBLEM OF A HYBRID DCT POWERTRAIN

Enrico Galvagno[1], Guido Guercioni[1], Giorgio Rizzoni[2], Mauro Velardocchia[1] and Alessandro Vigliani[1]*

[1] Politecnico di Torino, Dipartimento di Ingegneria Meccanica e Aerospaziale, corso Duca degli Abruzzi 24, 10129 Torino, Italy

[2] Ohio State University, Department of Mechanical and Aerospace engineering, 201 W 19th Ave, E329 Scott Lab, Columbus, OH 43210, USA

ABSTRACT– A Dynamic Programming (DP) formulation is developed to find the global optimal solution to the energy management of a parallel Plug-in Hybrid Electric Vehicle (PHEV) equipped with a Dual-Clutch Transmission (DCT).

The effects of integrating in the DP formulation the losses accounting for gearshifts and engine starts are studied in terms of the overall fuel consumption; the optimal control solutions obtained depends on the occurrence of these transient events. These sources of dissipation are modeled through physical considerations thus enabling the DP algorithm to decide when it is more convenient, in terms of minimizing the total energy consumption, to perform either a gearshift or an engine start. This capability differentiates the DP formulation here presented from those presented in previous studies.

KEY WORDS : Hybrid Electric Vehicle (HEV), Dual Clutch-Transmission (DCT), Energy Management Strategy (EMS), Dynamic Programming (DP)

NOMENCLATURE

a: vehicle acceleration

A_v: vehicle cross section

c_a: aerodynamic drag coefficient

c_r: rolling resistance coefficient

E: energy

f: generic function

F_a: aerodynamic resistance

F_g: slope gradient resistance

F_{in}: inertia force

F_r: rolling resistance

g: gravitational acceleration

GN: gear number

GS: gearshift

I: current

J: mass moment of inertia

M: vehicle mass

$\dot{m}_f$: fuel consumption

L: instantaneous cost function

r_w: wheel radius

P: power

R: electric resistance

Q: electric charge

QD_x: quick disconnect clutch status

SOC: state of charge

* *Corresponding author*. e-mail:
alessandro.vigliani@polito.it

t: time

T_s: time step

T: torque

TSF: torque split factor

u: command

U: commands domain

v: vehicle speed

V: voltage

W: lost power

x: state variable

X: state variables domain

Y: cost-to-go

α: road grade angle

Δx: range of state variables

ρ: air density

η: efficiency

Ψ: performance index

τ: transmission ratio

ω: angular speed

$\dot{\omega}$: angular acceleration

SUBSCRIPTS

B: battery

BR: mechanical brakes

EM: electric motor

GB: DCT gearbox

FD: final drive

INV: inverter

ICE: internal combustion engine

c: clutch

cd: cold start

chg: charge

co: Coulombic

cs: clutch slip

d: dissipated

dr: drag

dis: discharge

es: engine start

HS: half-shaft

i: input

$idle$: idle

in: inertia

k: time step

lim: limit

$loss$: loss

min: minimum

N: final step

OC: open circuit

max: maximum

n: oncoming

nom: nominal

o: output

p: offgoing

QD: quick disconnect

tgt: target

tot: total

u: command

w: wheel

1. INTRODUCTION

Hybrid Electric Vehicles (HEVs) are considered one of the most promising solutions to mitigate the environmental issues arising from the usage of fossil fuels in transportation systems (Böhme and Frank, 2017). In order to fully exploit the capabilities of these systems, a well-designed and properly tuned Energy Management Strategy (EMS) is of fundamental importance (Onori *et al*., 2016).

The energy management in HEVs consists in deciding the amount of power delivered at each time instant by the onboard energy sources (Onori *et al*., 2016; Guzzella and Sciarretta, 2013). Furthermore, depending on the powertrain architecture, a certain number of operational modes are available, e.g., EV-mode, ICE-only mode, Parallel hybrid mode, etc. The responsibility of deciding how and when to perform the transition among them, lies also with the EMS (Onori and Tribioli, 2015).

In order to fulfil the predefined control objectives, several model-based optimization methods have been explored to find the global optimal solution to the energy management problem in HEVs. These techniques, despite not being real-time implementable due to their preview nature and the computational burden involved (Salmasi, 2007), can provide engineers

with insights regarding how to fully take advantage of the capabilities of a certain powertrain. Dynamic Programming (DP) (Guzzella and Sciarretta, 2013; Kirk, 1998; Bellman and Dreyfus, 2015), Genetic Algorithms (GA) (Salmasi, 2007; Piccolo *et al*., 2001) and stochastic dynamic programming (Waschl *et al*., 2014; Johannesson *et al*., 2007) are numerical approaches that have been successfully implemented in previous works for the energy management of several different HEV powertrain architectures. On the other hand, among the analytical model-based techniques, Pontryagin's Minimum Principle (PMP) (Onori *et al*., 2016; Ostertag, 2011) is one of the most widely used approaches. It has been proved that, under certain conditions, PMP gives a non-causal solution which is globally optimal (Kim *et al*., 2011; Kim *et al*., 2012). In addition, researchers have recently shown interest in the use of convex optimization (Boyd and Vendenberghe, 2004; Elbert *et al*., 2014) since this approach can significantly reduce the computational time with respect to some numerical methods as DP. However, its use requires additional model approximations and discrete control variables, e.g., Internal Combustion Engine (ICE) state or the engaged gear number; thus it cannot be included in a convex formulation (Elbert *et al*., 2014).

DP is a numerical method to solve problems in which a sequence of interrelated decisions have to be taken (Bertsekas, 1995). A particular amount of attention has been given in literature to DP since is the only optimal control method capable of providing the optimal solution to problems of any complexity level within the accuracy limitations imposed by the discretization of problem variables (Onori *et al*., 2016). Hence, it allows generating benchmark solutions for real-time implementable EMSs (Lin *et al*., 2003; Ngo *et al*., 2013, Serrao *et al*., 2011). Furthermore, the results obtained with DP can be analyzed to extract rules allowing to generate a control trajectory similar to that of the global optimal solution to the control problem at hand (Lin *et al*., 2004; Bianchi *et al.*, 2010).

A common issue found in EMSs that do not explicitly incorporate drivability metrics in their performance index, is that the requests sent to the powertrain actuators aiming at optimizing the onboard energy consumption may have negative effects on vehicle drivability (Bovee, 2015, Galvagno *et al*., 2018). In particular, two of the most relevant kinds of decisions that can potentially cause drivability issues are high frequency switching among powertrain operating points/modes and frequent gearshifts (Opila *et al*., 2012a; Khodabakhshian *et al*., 2013).

Several research efforts have been dedicated to solving these issues using different approaches. In (Opila *et al*., 2009; Opila *et al*., 2012b) minimizing the overall number of ICE starts and gearshifts was included as one of the control objectives of a stochastic dynamic programming algorithm. Instead, in (Sciarretta *et al*., 2004) to prevent frequent ICE starts/stops as a result of implementing ECMS, the cost function is incremented considering the fuel equivalent energy (electrical energy used to power the starter) that is required to accelerate the ICE from rest to idle speed. In addition to the energy needed to go through the ICE start process, the energy losses of ICE starts and gearshifts are considered in (Ngo *et al*., 2012a) for a powertrain equipped with an Automated Manual Transmission (AMT) (Gao *et al*., 2011, Galvagno *et al*., 2014). To the best of the authors' knowledge, there are not yet available EMSs in which physical considerations are used to model the energy consumption during gearshifts for Dual-Clutch Transmissions (DCTs) (Galvagno *et al*., 2011; Galvagno *et al*., 2016; Guercioni, and Vigliani, 2019). If the ICE start losses are also properly modeled, this would allow to develop control strategies in which these maneuvers are undertaken when it is more convenient in terms of the overall energy consumption with the extra benefit of having an EMS in which transient events are not frequently requested, thus improving also the vehicle drivability. The authors are not aware of any other DP code that includes a similar modeling approach to account for the energy consumption of gearshifts in DCTs. Hence, the analysis of the optimal solution could give insights on how to improve the currently available real-time implementable EMSs.

In this paper a detailed DP formulation is developed for the energy management of a parallel Plug-in Hybrid Electric Vehicle (PHEV) equipped with a DCT. The main control objective is to minimize the total fuel consumption during a driving mission. To this end, five state variables are defined. This enables the DP algorithm to account for the gearshift and ICE start losses, the fuel cut-off functionality and to regulate the transition between the peak and continuous torque limits imposed to the Electric Machine (EM). Moreover, the importance of properly modeling the energy needed during the mentioned transient events is demonstrated by studying its effects on gear selection and ICE state variations.

The present paper is organized as follows. In section 2, the modeling work undertaken is addressed. The structure and capabilities of the studied PHEV are also described. Then, in the following two sections, the models developed to estimate the energy consumption during gearshifts and ICE starts are explained. In section 5, the optimal control problem formulation is given in a discretized form as it is solved by the DP algorithm; the introduction of the loss models developed for transient events is addressed in the subsequent section. Finally, simulation results are presented and analyzed in section 7.

2. POWERTRAIN DESCRIPTION AND MODELING

2.1. Powertrain description

The vehicle of interest corresponds to the parallel PHEV architecture depicted in Fig.1. The powertrain consists of an ICE, an EM, a battery pack and a DCT.

In the PHEV studied, the ICE and the EM are mounted on the same shaft, which is connected to the transmission input through the Dual Clutch Unit (DCU). Hence, it is possible to use them together or separately to propel the vehicle. Note that the ICE could produce additional power, with respect to the one required at the wheels, in order for the EM to use this extra energy to recharge the battery. As it is typical for hybridized powertrains, the introduction of the EM enables the possibility of performing regenerative braking. In addition, being this a PHEV, the battery cells can be recharged by an external power source.
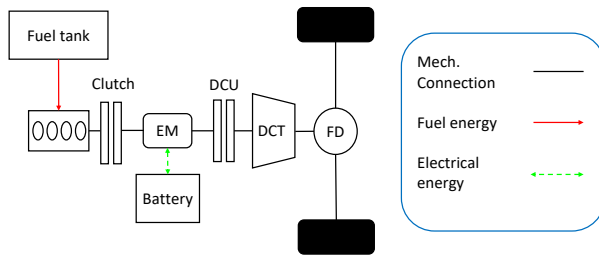

Figure 1. Powertrain layout.

A quick-disconnect dry clutch allows to separate the ICE from the wheels. This is particularly attractive when the powertrain operates in EV-mode since it allows the EM to propel the vehicle without having to drag the ICE inertia and compensate for its energy losses.
The most relevant powertrain components specifications are shown in Tab.1.

Table 1. Powertrain components.

Component	Data
Vehicle mass	1520 kg
ICE	Gasoline engine, 1.4 L, 110 kW
EM	75 kW (peak power)
DCT	6-speed transmission
Battery Pack	Li-ion, 8.8 kWh (26.5 Ah)

2.2. Powertrain model

2.2.1. Model overview

As common for simulators developed for energy management purposes, the main modeling objective is to reproduce the most relevant energy flows in the vehicle. A backward quasi-static approach (Guzzella and Sciarretta, 2013) is adopted here. No driver model is needed because the driving schedule is assumed to be followed exactly by the vehicle (Onori *et al.*, 2016). Quite obviously, this can be useful to assess and compare the performance of different EMSs since simulation results are computed for a vehicle that follows the same trace every time. However, when a backward simulator is employed, it is required to solve an implicit differential equation. Hence, backward-looking simulators are usually built using simplified models (Kim *et al.*, 2011). Fortunately, quasi-static models are appropriate for the development of EMSs, as shown in the literature (Rizzoni *et al.*, 1999; Guzzella and Amstutz, 1999). According to the quasi-static approach, the driving cycle is divided into small time intervals; then average values of speed, torque, and acceleration are considered. For the model at hand, a time step T_s of 1 s is selected, thus neglecting the dynamics faster than 1 Hz (Guzzella and Sciarretta, 2013; Ngo *et al.*, 2012b). The internal dynamics of powertrain components, e.g., ICE, half-shafts, etc., is much faster than that of the main energy flows and therefore they are neglected in the model.
Based on the powertrain architecture described in Fig.1, a model is developed in which the main inputs are:
- vehicle longitudinal speed
- vehicle longitudinal acceleration
- initial conditions for the state variables
- control inputs:
  - torque split factor
  - gear command
  - quick-disconnect clutch command
while the main outputs are:

- system states:
    - SOC
    - gear number
    - quick-disconnect clutch state
    - ICE state
    - EM torque counter state
- fuel consumption.

A description of the system states and control inputs is given in section 5.

2.2.2. Powertrain components

In this section, the modeling of the main powertrain components is described in detail.

2.2.2.1 Vehicle road load

If a vehicle is considered as a mass-point, the torque at the wheels T_w necessary to drive the system at a certain longitudinal speed v and acceleration a is:

$$T_w(t) = \left(F_r(t) + F_a(t) + F_{in}(t) + F_g(t) \right) r_w \qquad (1)$$

where r_w is the wheel radius.

The rolling resistance force is modeled as:

$$F_r(t) = c_r M g \cos \alpha(t) \qquad (2)$$

where c_r is the rolling resistance coefficient, $\alpha(t)$ is the road grade angle and M is the vehicle mass.

The aerodynamic drag force is computed as:

$$F_a(t) = \frac{1}{2} \rho A_v c_a v^2(t) \qquad (3)$$

where ρ is the air density, A_v is the vehicle frontal area and c_a is the aerodynamic drag coefficient.

Finally, the inertia force is:

$$F_{in}(t) = M a(t) \qquad (4)$$

while the slope gradient resistance $F_g(t)$ is

$$F_g(t) = M g \sin \alpha(t) \qquad (5)$$

In order to maximize the regenerative braking action, the torque request to the front axle, where the EM is connected, will be limited to avoid a demand higher than the value for which front wheel will lock-up occurs (Guiggiani, 2014).

2.2.2.2 DCT and differential

The PHEV is equipped with a 6-speed DCT with a layout similar to the one presented in (Galvagno *et al.*, 2016). For energy analysis, simple gear models that consider transmission ratios and constant efficiencies are employed (Guzzella and Sciarretta, 2013). Based on the previous considerations, the following speed relations can be established:

$$\omega_{GB,o}(t) = \omega_w(t) \tau_{FD} \qquad (6)$$
$$\omega_{GB,i}(t) = \omega_{GB,o}(t) \tau_{GB}(t) \qquad (7)$$

where $\omega_{GB,o}(t)$ and $\omega_{GB,i}(t)$ are respectively the angular speed at the DCT output and input shaft according to the engaged gear. Instead, $\omega_w(t)$ is the angular speed of the wheels, τ_{FD} is the final ratio and $\tau_{GB}(t)$ is the transmission ratio of the engaged gear.

Regarding the torque multiplication performed by DCT, it can be written:

$$T_{GB,i}(t) = \frac{T_w(t)}{\tau_{GB}(t)\tau_{FD}} \eta_{GB}^{z(t)} \eta_{FD}^{z(t)} \qquad (8)$$

where

$$z(t) = \begin{cases} -1 & \text{for } T_w \omega_w \geq 0 \\ 1 & \text{otherwise} \end{cases} \qquad (9)$$

where η_{GB} and η_{FD} are respectively the gearbox and final drive efficiency.

2.2.2.3 EM

A synchronous EM is modeled employing maps of torque and efficiency. The EM inertia is the only dynamic element considered. According to the quasi-static approach, the inertia torque is calculated at each time step based on an average value of the vehicle acceleration as:

$$T_{EM,in}(t) = \dot{\omega}_{EM}(t) J_{EM} \qquad (10)$$

where $\dot{\omega}_{EM}$ is the EM angular acceleration and J_{EM} represents its mass moment of inertia.

When a gearshift maneuver is not performed, the EM speed is assumed equal to the input speed of the DCT, which is directly linked to the wheel speed through Eq. (6) and (7), i.e.:

$$\omega_{EM}(t) = \omega_w(t) \tau_{GB}(t) \tau_{FD} \qquad (11)$$

On the other hand, the average EM speed during gearshift is estimated in a different manner, as discussed in section 3.

The efficiency of the EM is interpolated from the mentioned maps as a function of the EM speed $\omega_{EM}(t)$ and torque request $T_{EM}(t)$:

$$\eta_{EM}(t) = f\big(\omega_{EM}(t), T_{EM}(t) \big) \qquad (12)$$

Moreover, a series of torque and speed limitations must be respected, i.e.:

$$T_{EM,min}(t) \leq T_{EM}(t) \leq T_{EM,max}(t) \qquad (13)$$
$$\omega_{EM,min} \leq \omega_{EM}(t) \leq \omega_{EM,max} \qquad (14)$$

The maximum and minimum value to be considered for the EM torque request are interpolated as a function of angular speed:

$$T_{EM,max}(t) = f\left(\omega_{EM}(t), \mathrm{T}_{EM,lim}(t) \right) \qquad (15)$$

$$T_{EM,min}(t) = f\left(\omega_{EM}(t), \mathrm{T}_{EM,lim}(t) \right) \qquad (16)$$

where $\mathrm{T}_{EM,lim}(t)$ is a counter used to select whether to enforce the peak or the continuous EM torque limit (see section 5).

Finally, the EM power can be computed as described in Eq.(17). Note that, for convenience, all the other sources of energy consumption in the electrical path are included in the expression. This implies that Eq. (17) can also be regarded as the power request at battery terminals $P_B(t)$.

$$P_{EM}(t) = P_B(t) = T_{EM}(t)\, \omega_{EM}(t)\, \eta_{EM}(t)^{z(t)} \eta_{inv}^{z(t)} + P_{DC/DC} + P_{d,DCT}(t) \qquad (17)$$

$$P_{d,DCT}(t) = \begin{cases} \bar{P}_{d,DCT} + P_{d,GS} & \text{for } GS = 1 \\ \bar{P}_{d,DCT} & \text{for } GS = 0 \end{cases} \qquad (18)$$

where GS is the gearshift status, which is equal to 1 when a gearshift is performed, otherwise, it is set to 0;

η_{INV} is the inverter efficiency and $P_{DC/DC}$ is the power of the DC/DC converter. Furthermore, from an experimental assessment of the power consumption of the DCT actuation system, it was concluded that the electric power required during vehicle operation could be approximated by an average drawn power $\bar{P}_{d,DCT}$ and a component that is considered only when a gearshift is performed $P_{d,GS}$.

2.2.2.4 Battery

The State Of Charge (SOC) is defined as the amount of electric charge stored in the battery $Q(t)$ relative to the total charge capacity Q_{nom}:

$$SOC(t) = \frac{Q(t)}{Q_{nom}} \qquad (19)$$

The SOC dynamics is given by:

$$\frac{d}{dt}SOC(t) = \frac{\dot{Q}(t)}{Q_{nom}} = -\frac{I(t)}{Q_{nom}} \qquad (20)$$

Since the current $I(t)$ is considered positive during discharge, the minus sign in the former equation accounts for the expected reduction in SOC.

For HEVs energy management, a control-oriented zero-th order equivalent circuit model (Guzzella and Sciarretta, 2013) has been widely used in literature (Onori and Tribioli, 2015; Kim *et al*., 2011). According to this model, the battery voltage can be written as:

$$V_B(t) = V_{OC}(SOC(t)) - R_B(SOC(t))I(t) \qquad (21)$$

where $V_{OC}(SOC(t))$ is the battery Open Circuit (OC) voltage and $R_B(SOC(t))$ is the battery internal resistance.

Hence, the current is expressed as a function of battery power, yielding:

$$I(t) = \eta_{co}\frac{V_{OC}(SOC(t)) - \sqrt{V_{OC}^2(SOC(t)) - 4P_B(t)R_B(SOC(t))}}{2R_B(SOC(t))} \qquad (22)$$

where η_{co} is the coulombic efficiency and $P_B(t)$ is the power at battery terminals.

The physical limits of the battery must be included in the model in order for it to be used for control purposes. The maximum discharge power can be expressed according to (Guzzella and Sciarretta, 2013):

$$P_{B,max}(SOC(t)) = \frac{V_{OC}^2(SOC(t))}{4R_B(SOC(t))} \qquad (23)$$

Instead, the battery power during charging is limited imposing a maximum value $V_{B,max}$ for the voltage which can be seen in terms of a minimum charge current as:

$$I_{min}(SOC(t)) = \frac{V_{OC}(SOC(t)) - V_{B,max}}{R_B(SOC(t))} \qquad (24)$$

As it can be appreciated in the former set of equations, both the OCV and the battery internal resistance are modeled as a function of the SOC (Onori and Tribioli, 2015; Kim *et al*., 2011). The internal resistance of the battery pack can be calculated as:

$$R_B(SOC(t)) = \begin{cases} R_{B,dis}(SOC(t)) & \text{for } P_B \geq 0 \\ R_{B,chg}(SOC(t)) & \text{otherwise} \end{cases} \qquad (25)$$

where $R_{B,dis}(SOC(t))$ and $R_{B,chg}(SOC(t))$ are respectively the battery pack internal resistance during discharge and charge.

Similar to the resistance, for the OCV, it can be written that:

$$V_{OC}(SOC(t)) = \begin{cases} V_{OC,dis}(SOC(t)) & \text{for } P_B \geq 0 \\ V_{OC,chg}(SOC(t)) & \text{otherwise} \end{cases} \qquad (26)$$

where $V_{OC,dis}(SOC(t))$ is the OCV of battery cells during discharge and $V_{OC,chg}(SOC(t))$ represents the same quantity during charge.

2.2.2.5 ICE

As for the EM, the ICE is modeled using torque and efficiency maps and the only dynamic element considered is the ICE inertia J_{ICE}. The torque needed to accelerate the ICE is computed as:

$$T_{ICE,in}(t) = \dot{\omega}_{ICE}(t)J_{ICE} \qquad (27)$$

When the quick-disconnect clutch is engaged, the ICE speed is assumed equal to that of the EM, i.e., $\omega_{ICE}(t) = \omega_{EM}(t)$. However, during ICE start events, the average speed considered is calculated in a different manner, as discussed in section 4.

The efficiency of the ICE is represented by means of the fuel consumption map as a function of the ICE speed ω_{ICE} and torque request T_{ICE}:

$$\dot{m}_f(t) = f(\omega_{ICE}(t), T_{ICE}(t)) \qquad (28)$$

As for the EM the physical torque and speed limitations of the ICE are considered, i.e.:

$$T_{ICE,max}(t) = f(\omega_{ICE}(t)) \qquad (29)$$
$$T_{ICE,dr}(t) = f(\omega_{ICE}(t)) \qquad (30)$$

3. DCT GEARSHIFT LOSSES MODELING

3.1. Model overview

The estimation of the energy losses associated to gearshifts relies on a simplified model of the powertrain, thus allowing to quantify energy dissipation without considerably increasing the computational effort. The losses computed with this model depend on the powertrain/transmission architecture, operating modes, component parameters (inertia, ICE drag, etc.) and maneuver.

In particular, it is worth mentioning that when solving the optimal control problem by means of DP, several solution candidates are tested at each iteration; therefore, it is convenient to have tools that allow performing each of these calculations as fast as possible while maintaining the desired level of accuracy.

A summary of the main inputs and outputs of the model developed to estimate the gearshift losses is presented below.

Main inputs:

- torque request at the wheels
- vehicle speed
- vehicle acceleration
- oncoming gear number
- offgoing gear number

Main outputs:

- EM speed
- total torque request to powertrain components.

3.2. Energy request calculation

The speed profiles of the EM and the two clutches togheter with each clutch torque profile are assumed to be known inputs for the expressions presented in this section.

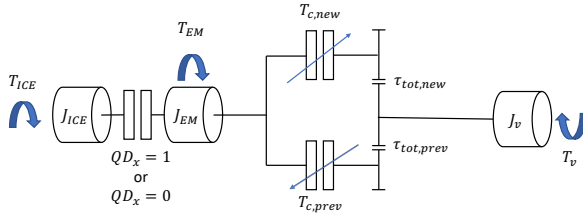The simplified powertrain model for energy analysis used is shown in Fig.2.

Figure 2. Powertrain model: gearshifts energy request.

Based on the developed model, the total torque passing through the DCU $T_c(t)$ and the torque applied to the wheels $T_{HS}(t)$ can be written as:

$$T_c(t) = T_{c,p}(t) + T_{c,n}(t) \qquad (31)$$
$$T_{HS}(t) = T_{c,p}(t)\,\tau_{tot,p}(t) + T_{c,n}(t)\,\tau_{tot,n}(t) \qquad (32)$$

with

$$\tau_{tot,p}(t) = \tau_p(t)\tau_{fd} \qquad (33)$$
$$\tau_{tot,n}(t) = \tau_n(t)\tau_{fd} \qquad (34)$$

where, $T_{c,p}(t)$ and $T_{c,n}(t)$ are respectevely the torque passing by the offgoing and oncoming clutch. Acoordingly, $\tau_p(t)$ is the transmission ratio of the offgoing gear and $\tau_{tot,n}(t)$ represents the same variable but for the oncoming gear.

Moreover, the total inertia torque considered depends on whether or not the quick-disconect clutch status QD_x is open ($QD_x = 0$) or closed ($QD_x = 1$), thus it can be written:

$$T_{in,tot}(t) = \begin{cases} T_{ICE,in}(t) + T_{EM,in}(t) & \text{for } QD_x = 1 \\ T_{EM,in}(t) & \text{otherwise} \end{cases} \qquad (35)$$

From the power equilibrium at the two clutches, the following expressions are found:

$$T_{c,p}(t)\omega_{EM}(t) = T_{c,p}(t)\omega_{c,p}(t) + W_{c,p}(t) \qquad (36)$$
$$T_{c,n}(t)\omega_{EM}(t) = T_{c,n}(t)\omega_{c,n}(t) + W_{c,n}(t) \qquad (37)$$

Note that in Eq. (6) and (7) the fact that $\omega_{EM}(t) \neq \omega_{c,j}(t)$ implies that a certain amount of energy is dissipated. Hence, $W_{c,p}(t)$ and $W_{c,n}(t)$ represent the slip power losses of each of the two clutches which in general can be computed based on the clutch slip velocity $\omega_{cs}(t)$ as:

$$W_{cs}(t) = \omega_{cs}(t)T_c(t) \qquad (38)$$

Finally, the total power request can be expressed as:

$$P_{tot,GS}(t) = T_{in,tot}(t)\omega_{EM}(t) \qquad (39)$$

and the total energy request is determined by integration:

$$E_{tot,GS}(t) = \int_0^{T_s} P_{tot,GS}(t)\, dt \qquad (40)$$

Based on the overall energy needed to perform the gearshift maneuver, a mean torque request is elaborated and sent to the EMS, with the task of deciding how to divide it among the onboard power generation devices. Hence, the total torque request is:

$$T_{tot,GS}(t) = \frac{E_{tot,GS}(T_s)}{\bar{\omega}_{EM}T_s} \qquad (41)$$

where $\bar{\omega}_{EM}$ is the mean speed of the EM during the gearshift process.

3.3 Simulation results

The gearshift process is here simplified to obtain the torque and speed profiles for the DCT components allowing to easily compute the energy consumption resulting from upshift and downshift maneuvers.

3.3.1 Downshifts

Figure 3 illustrates a 2nd to 1st downshift process. Since shafts are assumed to be perfectly rigid, the velocity of both clutches is given by the wheel speed. Furthermore, another linear profile is assumed for the EM shaft (DCU input shaft) considering that, at the end of the inertia phase, its speed increases until a small positive slip velocity (5 rad/s) is reached. This allows to transmit positive power through both clutches during the torque phase.
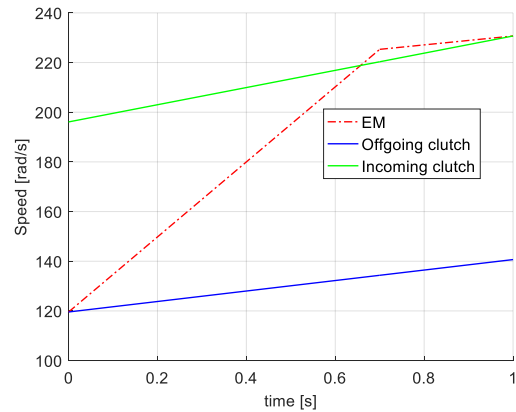

Figure 3. Gearshift speed profiles: downshift.

On the other hand, in Fig.4 the torque passing through the clutches is presented. During the inertia phase, the oncoming clutch is completely disengaged, and the torque requested at the wheels is transmitted by the offgoing clutch. Instead, during the torque phase, the latter is completely disengaged while the other is closed. Note that the torque trajectories assumed for the second part of the gearshift process are computed in order to satisfy the power request at the wheels at all times.
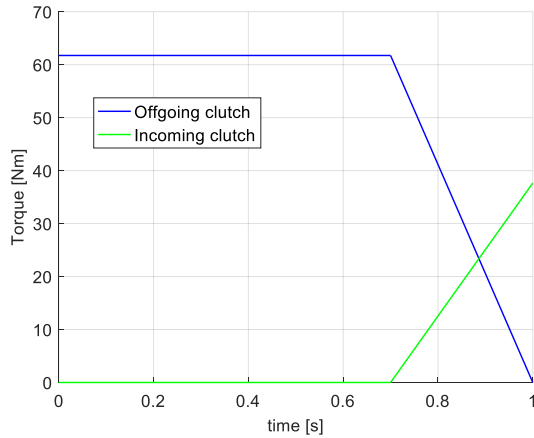

Figure 4. Gearshift torque profiles: downshift.

3.3.2 Upshifts

Figure 5 shows a 1st to 2nd upshift maneuver. Again, the velocity of the clutches can be estimated based on the wheel speed. During the torque phase, a small constant positive slip velocity (5 rad/s) is assumed for the EM shaft. Once the offgoing clutch is fully disengaged (see Fig. 6), this speed is set to decrease linearly until it matches that of the oncoming clutch.
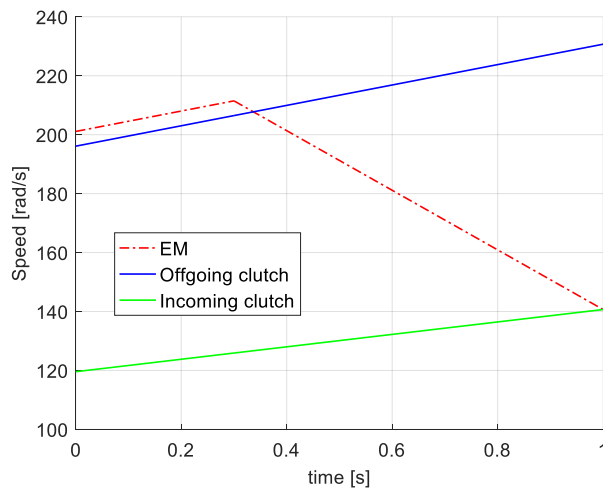

Figure 5. Gearshift speed profiles: upshift.

Besides the fact that the torque and inertia phase occur in a different order, the same considerations made for

downshifts regarding the torque passing through the clutches still apply. Figure 6 presents the assumed torque profiles.
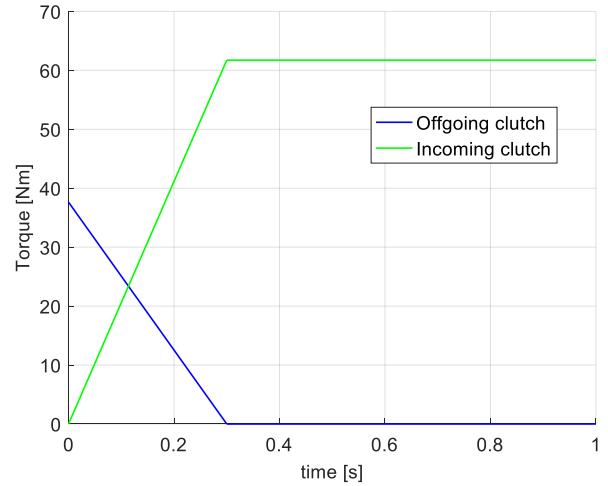

Figure 6. Gearshift torque profiles: upshift.

Figure 7 illustrates how the energy necessary to undertake the gearshift process is distributed. It can be appreciated that the amount of energy dissipated due to clutch slip is not negligible. Moreover, note that the need to decrease the speed of the EM shaft helps reducing the total energy requested.
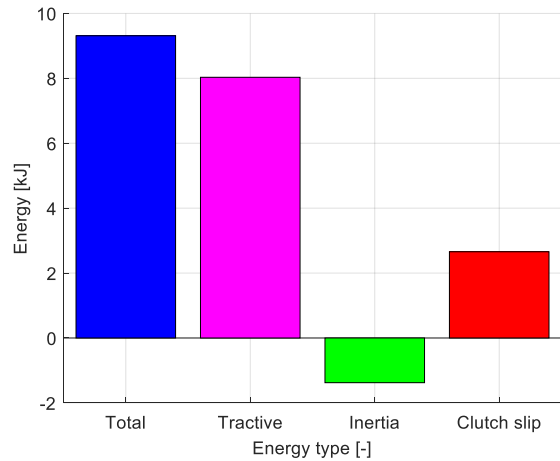

Figure 7. Gearshift energy: upshift.

4. ICE START LOSSES MODELING

4.1. Model overview

An approach similar to the one proposed in (Ngo *et al*., 2012a) is used to estimate the amount of energy employed during ICE start events. The modeling of the energy required to start the ICE is performed with the objective of integrating this calculation into EMSs for

HEVs. Hence, the level of complexity of the computations involved is limited, based on a compromise between the necessity of evaluating several solution candidates to the energy management problem and the purpose of properly estimating the amount of energy being used.

The ICE start losses calculation is performed dividing the whole process into two consecutive phases:

- phase I: acceleration of the ICE to idle speed
- phase II: ICE and EM speed matching

Each of these phases is addressed in the next paragraph. For simplicity, the following assumptions are made for ICE starts:

- there will be no gearshift at the same time step in which the ICE is started
- the ICE cannot be used to satisfy the torque request at the wheels during its start process.

For the estimation of the ICE start losses, the main inputs are:

- vehicle speed
- vehicle acceleration
- gear number

while the main outputs are:

- ICE speed
- torque request to ICE
- extra torque request to EM.

4.2 ICE start phases

As for the gearshift losses modeling, assumptions are made regarding the speed profiles of the powertrain components (see section 4.4). For this reason, the speed of the ICE and the EM are considered as inputs for the equations presented here.

4.2.1 Phase I: accelerate the ICE to idle speed

Since the HEV is not equipped with a conventional starter, the ICE needs to be accelerated by the torque passing trough the quick-disconet clutch until its minimum speed is reached. This implies that the EM has to provide the necessary power ($P_{ICE}(t) = 0$ during this phase).

A positive slip velocity in the quick-disconnect clutch is assumed when the EM is spining faster than the ICE. Since the ICE is off, its dynamics is given by:

$$J_{ICE}\dot{\omega}_{ICE}(t) = T_{QD}(t) - T_{ICE,dr}(t) \qquad (42)$$

Considering that the quick-disconet clutch is slipping during this phase, the following expression holds for the torque transmitted through it:

$$T_{QD}(t) = T_{o,QD}(t)\,\text{sign}(\omega_{EM}(t) - \omega_{ICE}(t)) \qquad (43)$$

with $T_{o,QD}(t)$ being the clutch transmissible torque.

From the power equilibrium at the quick-disconet clutch, the power loss due to clutch slipping can be computed from:

$$T_{QD}(t)\omega_{EM}(t) = T_{QD}(t)\omega_{ICE}(t) + P_{QD,loss}(t) \qquad (44)$$

The extra power request to the EM (to be added to the torque needed to propel the vehicle) is determined using the next expression, in which $T_{QD}(t)$ is calculated from Eq.44, based on the speed profile assumed for the ICE.

$$P_{EM,es}(t) = T_{QD}(t)\omega_{EM}(t) \qquad (45)$$

4.2.2 Phase II: ICE and EM speed match

At the beginning of phase II the ICE has reached its idle speed; then it is controlled to match its speed with the EM. Hence, its dynamics is described as:

$$J_{ICE}\dot{\omega}_{ICE}(t) = T_{QD}(t_I) + T_{ICE}(t) - T_{ICE,dr}(t) \qquad (46)$$

with t_I being the time length of phase I.

The transmissible torque of the quick-disconnect clutch is kept constant until the speed of the EM and the ICE are equal, then it is fully closed. Therefore, the power requests to the system prime movers are:

$$P_{ICE}(t) = T_{ICE}(t)\omega_{ICE}(t) \qquad (47)$$
$$P_{EM,es}(t) = T_{QD}(t_I)\omega_{EM}(t) \qquad (48)$$

where $T_{ICE}(t)$ is computed using Eq.(46).

In case the torque passing through the clutch at the end of phase I is higher than the torque required for the speed match, instead of opening the clutch again (to keep $T_{ICE}(t)$ higher than zero), the ICE start process is undertaken using the EM, i.e.:

$$J_{ICE}\dot{\omega}_e(t) = T_{QD}(t) - T_{ICE,dr}(t) \qquad (49)$$
$$P_{ICE}(t) = 0 \qquad (50)$$
$$P_{EM,es}(t) = T_{QD}(t)\omega_{EM}(t) \qquad (51)$$

4.3 Energy request calculation

In addiction to the power requested at the wheels, a certain amount of energy is needed from the EM during ICE starts that can be estimated as:

$$E_{EM,es}(t) = \int_0^{T_s} P_{EM,es}(t)\,dt \qquad (52)$$

from which a mean torque is computed:

$$T_{EM,es}(t) = \frac{E_{EM,es}(T_s)}{T_s\,\bar{\omega}_{EM}} \qquad (53)$$

where $\bar{\omega}_{EM}$ is the mean speed of the EM that can be derived from the wheel speed through the total gear ratio.

On the other hand, the total energy request to the ICE is:

$$E_{ICE}(t) = \int_0^{T_s} P_{ICE}(t)\,dt \qquad (54)$$

The mean total torque request to the ICE is then:

$$T_{ICE}(t) = \frac{E_{ICE}(T_s)}{T_s\,\bar{\omega}_{ICE}} \qquad (55)$$

where $\bar{\omega}_{ICE}$ is the mean speed of the ICE during the start process.

4.4 Simulation results

Firstly, an ICE start process in 2nd gear is described. Figure 8 shows the speed profiles of the ICE and EM. For the ICE, a linear speed trajectory is assumed, that goes from zero to idle speed during phase I and then from idle to the EM speed.
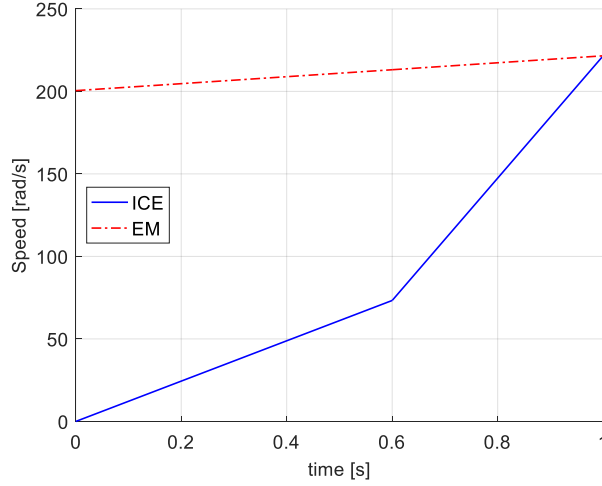

Figure 8. ICE start speed profiles.

Figure 9 shows how the total energy request is being distributed. The EM provides most of the energy while the ICE is used only in phase II. As in the gearshift simulation results, the energy dissipation due to clutch slip is not negligible.
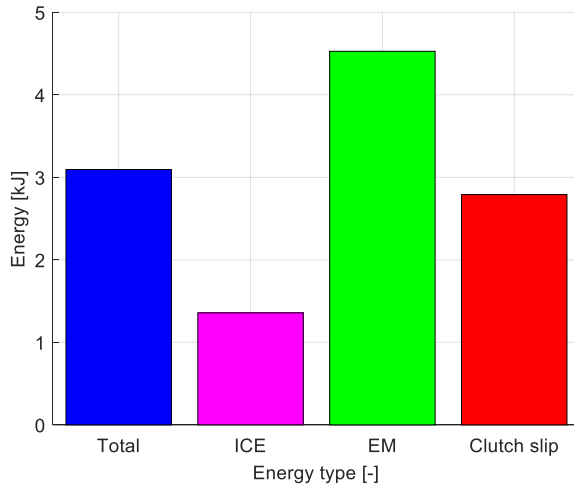

Figure 9. ICE start energy.

5. OPTIMAL CONTROL PROBLEM FORMULATION

In this section, the general problem formulation used to find the global optimal solution to the energy management of the HEV powertrain architecture described in section 2 is given in a discretized form as it is solved by the DP algorithm.

The constrained-finite time horizon optimal control problem can be formally defined as finding the control sequence that minimizes the performance index of interest while meeting a specified set of constraints, i.e., dynamic state, global state, local state and control constraints.

To accomplish this task, state x_k and control u_k variables have to be defined, bounded and discretized. This implies that the powertrain model must be expressed as a discrete-time system:

$$x_{k+1} = f_k(x_k, u_k) \qquad (56)$$

Note that Eq. (56) represents the dynamic state contraints of the problem, where k takes integer values and indicates the current time step.

Moreover, local contraints are also defined, meaning that the state and control variables can only assume values contained in their respective domains X_k and U_k.

$$x_k \in X_k \qquad (57)$$
$$u_k \in U_k \qquad (58)$$

Finally, the last type of contraints that need to be reported are the global state contraints. These are usually used to enforce a desired final value x_{tgt} or an acceptable range Δx around it for the state variables:

$$x_N - x_{tgt} = \pm\Delta x \qquad (59)$$

Having defined a discrete representation of the system to be controlled toghether with its boundaries, let us consider a generic performance index, given as a function of the initial states x_0 and the control policy u:

$$\Psi(x_0, u) = L_N(x_N) + \sum_{k=1}^{N-1} L_k \qquad (60)$$

where L_k is the instantaneous cost function, or arc cost in the context of DP, and L_N is the terminal cost at the final time step N wich depends on the final state x_N, e.g., when the final state is constrained, control candidates that lead to state variables values outside the allowable range are assigned an infinite cost.

The optimal control problem of interest is now fully described in a discretized form by Eq. (56-60) and can be solved using numerical methods as DP. The main advantage of DP lies on the fact that is able to handle nonlinearity and discrete variables within the problem formalization while obtaining a globally optimal solution (Lin *et al.*, 2003). This technique is based on Bellman's principle of optimality according to which: an optimal control policy has the property that from any point on an optimal trajectory, the remaining trajectory is optimal for the sub-problem initiated at that point (Onori *et al.*, 2016). The fundamental implication of this statement, is that the overall optimal control policy can be obtained solving a sequence of simpler minimization problems proceding backwards (Lin *et al.*, 2003). This

can be achieved by generating at each step the optimal cost-to-go Y_k^*:

For $k = N - 1$:

$$Y_{N-1}^* = \min_{u \in U_k}\big(L_{N-1}(x_{N-1}, u) + L_N(x_N)\big) \qquad (61)$$

Instead, for $1 \le k < N - 1$:

$$Y_k^* = \min_{u \in U_k}\big(L_k(x_k, u) + Y_{k+1}(f_k(x_k, u_k), u_k)\big) \qquad (62)$$

where Y_k^* represents the optimal cost-to-go from state x_k (at time k) to the end of the optimization horizon. Note that Y_{k+1} is the optimal cost-to-go from the resulting state $x_{k+1} = f_k(x_k, u_k)$ after applying a certain control u_k.

The implementation and solution of the recursive equations presented above for the optimal control problem formulation described in this section will be undertaken using a general-purpose DP algorithm. The reader is referred to (Sundström and Guzzella, 2009) for a detailed description of the mentioned software.

In the next paragraphs, specific definitions for the arc-cost, state and control variables and their boundaries will be provided.

5.1 Cost function

The control objective is to minimize the overall fuel consumption during a certain driving cycle. The instantaneous cost function, or arc cost, is thus defined:

$$L_k = \dot{m}_{f,tot,k} \qquad (63)$$

where $\dot{m}_{f,tot,k}$ is the total fuel consumption rate which considers the fuel penalties discussed in section 6.4.

5.2 States and constrains

In the DP formulation developed, a total of five state variables are defined together with a series of local and global state constrains.

In general, when minimizing the overall fuel consumption is the main control objective, the battery SOC is used as the only state variable. However, when solving an optimal control problem by means of DP, the only way to pass information from one iteration to the next is using state variables. As a consequence, for the DP solution to account for the gearshift and ICE start losses, the fuel cut-off functionality and the limitation described in section 2.2.2.3 regarding the EM torque, four additional state variables are needed. Adding this level of detail reagarding powertrain modeling and operating modes into the DP formulation allows to obtain more physically correct solutions to the energy management problem which can give a better understanding of the maximum powertrain capabilities and how to achieve them in terms of control.

The price to pay for this improved level of accuracy is a higher computational burden of the calculations, that increases linearly with the final time and exponentially with the dimension of the state vector. This is referred to in literature as the curse of dimensionality (Kirk, 1998). This was seen during the development of the algoritnm during which simulation times increased from a few hours to almost an entire day with the progressive addition of state variables. However, optimizing the simulation time is out of the scope of this paper. The reader is reffered to (Ngo et al., 2012a) for further information on a DP based approach aiming to achieve near-optimal results while reducing the computational effort.

5.2.1 SOC

Since the SOC is a dynamic variable, it is defined as a state. Estimating the value of the SOC at each iteration enables the algorithm to account for the physical limitations of the energy storage system and to impose a final target for it.

The SOC is defined using a discretized version of Eq. (20)

$$SOC_k = SOC_{k-1} - \frac{I_k}{Q_{nom}} T_s \qquad (64)$$

According to the characteristics of the energy storage system present in the vehicle, the local state constrains are defined as:

$$SOC_k \in [0.32, 0.93] \qquad (65)$$

As a consequence, the initial and final SOC values must belong to the range defined in Eq. (65)

5.2.2 Gear number

In order to introduce the modeling of the gearshift losses into the DP formulation, the gear number is defined as a state. In this way, by comparing the value of this variable at the previous iteration with the gear command being given at the current step, gearshift maneuvers are detected, and the corresponding losses can be estimated.

For the gear number, the state dynamics depends only on the control inputs:

$$GN_{x,k} = GN_{u,k} \qquad (66)$$

where $GN_{u,k}$ is the gear command.

Since the PHEV is equipped with a 6-speed DCT, seven discrete values are possible for the gear number state:

$$GN_{x,k} \in [0, 6] \qquad (67)$$

The neutral gear ($GN_x = 0$) is forced when the torque request to the vehicle is zero. For the gear number, there are no boundary conditions.

5.2.3 Quick-disconnect clutch state

In order to introduce the modeling of the ICE start losses, the quick-disconnect clutch state is defined. In this way, by comparing the value of this variable at the previous iteration with the clutch command being given at the current step, ICE start maneuvers are detected, and the corresponding losses can be estimated. Note that each time the quick-disconnect clutch state passes from

disengaged to engaged, an ICE start is undertaken. Obviously, the quick-disconnect clutch state is a binary variable that can assume one of two values: open ($QD_{x,k} = 0$) or closed ($QD_{x,k} = 1$).

As for the gear number, the state dynamics depends only on the control inputs:

$$QD_{x,k} = QD_{u,k} \tag{68}$$

where $QD_{u,k}$ is the quick-disconnect clutch command. For this state, there are no boundary conditions.

5.2.4 ICE state

Similar to the quick-disconnect clutch state, the ICE state is a binary variable that can assume one of two values: off ($ICE_{x,k} = 0$) or on ($ICE_{x,k} = 1$).

The ICE state is determined by the torque request resulting from the torque split control input:

$$ICE_{x,k} = \begin{cases} 1 \text{ for } T_{ICE,k} > 0 \\ 0 \text{ otherwise} \end{cases} \tag{69}$$

where $T_{ICE,k}$ is the torque request to the ICE decided by the EMS. For this state, there are no boundary conditions.

The reason behind the definition of this state is that the quick-disconnect clutch status is not enough to determine if the ICE is being used, since the fuel cut-off functionality is introduced, i.e., it is possible to turn off the ICE without opening the quick-disconnect clutch, and therefore, without having to perform an ICE start event the next time this component is needed.

5.2.5 EM torque counter state

As anticipated in section 2.2.2.3, a counter is needed to establish whether to enforce the continuous or peak torque limit when defining the set of admissible control inputs to the EM. In particular, from experimental experience it was determined that if the continuous torque limit is breached for 7 consecutive seconds, at least 13 s must pass before the EM torque can go again above its continuous boundary. This condition is set to ensure that the EM components operate on a desirable temperature range.

Hence, a counter is designed, in which each time the torque request is within the continuous limit and its value is lower than 7, a reset is enforced. On the other hand, when the counter reaches a value of 7, it is reset only after 13 additional time steps have passed. Based on the previous considerations, the following local conditions are established:

$$T_{EM,lim,k} \in [0, 20] \tag{70}$$

Quite obviously, the initial value of this state is equal to zero.

The discretization of state variables is as follows:
- State Of Charge: $\Delta SOC_k = 0.1\%$
- Gear number: $\Delta GN_{x,k} = 1$
- Quick-disconnect clutch state: $\Delta QD_{x,k} = 1$

- ICE state: $\Delta ICE_{x,k} = 1$
- EM torque counter state: $\Delta T_{EM,lim,k} = 1$

5.3 Controls and constrains

In the following, the physical meaning of each control variable is addressed and the local control constrains are reported.

5.3.1 Torque split factor

The Torque Split Factor (TSF) is a control variable introduced to indicate how the total power request at the wheels is distributed between the ICE and the EM. It is defined as the ratio between the EM torque request T_{EM_k} and the total torque request at the transmission input T_{tot_k}:

$$TSF_k = \frac{T_{EM_k}}{T_{tot_k}} \tag{71}$$

The local constrains on the TSF are:

$$TSF_k \in [-1, 1] \tag{72}$$

Given the definition presented in Eq.71, the physical meaning of the values the TSF can take is summarized as:
- $TSF_k = 1$ implies operation in EV-mode
- $TSF_k \in (0,1)$ implies operation in parallel hybrid mode
- $TSF_k = 0$ implies operation in ICE-only mode
- $TSF_k \in [-1,0)$ implies operation in hybrid mode. In this case, additional torque, with respect to the torque requested for traction, is supplied by the ICE to recharge the battery and/or optimize its operating point. In theory, the amount of torque available to recharge the battery is only bounded by the physical limitations of powertrain components. For the simulations presented, the value of -1 is used, implying that the torque available for battery recharge can be high as the one requested to satisfy the wheel torque request. It is worth mentioning that the lower boundary of the TSF was only reached in a few occasions in the simulations performed.

5.3.2 Gear command

At each time step, the EMS must select the engaged gear of the DCT. There are six possible gears to choose from:

$$GN_{u,k} \in [1, 6] \tag{73}$$

As explained for the gear number state, the neutral position is enforced based on the torque request at the wheels.

5.3.3 Quick-disconnect clutch command

According to the definition given for the quick-disconnect clutch state in section 5.2.3, the corresponding control is also a binary variable that can

assume one of two values: 0 or 1. The physical meaning of those values is:

- $QD_{u,k} = 1$ implies that the clutch is closed or kept closed.
- $QD_{u,k} = 0$ implies that the clutch is open or kept open.

6. INTRODUCTION OF GEARSHIFT AND ICE START LOSSES

This section describes how the gearshift and ICE start losses are integrated into the DP formulation. In particular, the computation of the total torque request to powertrain actuators and its distribution among the ICE and the EM are described while explaining how the outputs of the mentioned loss models are employed.

6.1 Total torque request

The generic expression for computing the torque request at the transmission input shaft when there is no gearshift is:

$$T_{tot,nGS,k} = T_{ICE,in,k} + T_{ICE,dr,k} + T_{EM,in,k} + T_{GB,i,k} \quad (74)$$

The ICE drag torque and its inertia are considered only when the quick-disconnect clutch is closed and when an ICE start is not being undertaken, since these contributions are already considered in the ICE start loss model. Hence, when either of the mentioned conditions are not verified:

$$T_{tot,nGS,k} = T_{EM,in,k} + T_{GB,i,k} \quad (75)$$

On the other hand, when a gearshift event occurs, the total torque request at the EM shaft is computed based on the output of the DCT gearshift loss model. Therefore, in general, it can be written:

$$T_{tot,k} = \begin{cases} T_{tot,nGS,k} & \text{for } GS_k = 0 \\ T_{tot,GS,k} & \text{for } GS_k = 1 \text{ and } QD_{u,k} = 0 \\ T_{tot,GS,k} + T_{ICE,dr,k} & \text{for } GS_k = 1 \text{ and } QD_{u,k} \neq 0 \end{cases} \quad (76)$$

where $T_{tot,GS,k}$ is the total torque request during gearshift maneuvers, i.e., the output of the gearshift loss model presented in section 3. Note that the ICE drag torque is added to this quantity since it is not considered when generating $T_{tot,GS,k}$.

6.2 Torque request to ICE

The ICE torque request is elaborated based on the TSF and the ICE start status. It is assumed that the ICE will be requested to provide positive torque. Therefore, considering the TSF, it can be written:

$$T_{ICE,k} = \begin{cases} T_{tot,k}(1 - TSF_k) & \text{for } T_{tot,k} > 0 \\ 0 & \text{otherwise} \end{cases} \quad (77)$$

where $T_{ICE,k}$ is the torque request to the ICE.

On the other hand, in case of a negative request to the thermal path, mechanical braking is employed:

$$T_{BR,k} = \begin{cases} T_{tot,k}(1 - TSF_k) & \text{for } T_{tot,k} < 0 \\ 0 & \text{otherwise} \end{cases} \quad (78)$$

where $T_{BR,k}$ is the torque request to the mechanical brakes reported at the EM shaft.

However, in case of an ICE start, the ICE torque request and angular speed are overwritten by the outputs of the ICE start loss model.

6.3 Torque request to EM

Similar to the ICE torque request, the torque that the EM must provide is computed based on the TSF and the ICE start status.

Considering the extra torque request computed by the ICE start loss model (see Eq.55), the EM torque is:

$$T_{EM,k} = \begin{cases} T_{tot,k}TSF_k & \text{for } es_k = 0 \\ T_{tot,k}TSF_k + T_{EM,es,k} & \text{otherwise} \end{cases} \quad (79)$$

where $T_{EM,es,k}$ is the additional torque request to the EM computed by the ICE start loss model.

When there is an ICE start, i.e., the state of the quick-disconnect clutch goes from open to closed, the ICE start status es_k is 1, otherwise, it is set to 0.

6.4 Introduction of fuel penalties

As stated in section 5.2.4, the introduction of a state variable for the ICE allows the developed DP formulation to account for the possibility of not utilizing this component even when the quick-disconnect clutch is closed, which it is referred to as fuel cut-off functionality.

To account for the fact that the ICE will cool down during the time steps in which there is a fuel cut-off or when the quick-disconnect clutch is disengaged, meaning that an extra quantity of fuel will have to be used to compensate for it, a fuel penalty is introduced. For simplicity, a constant value is considered.

Therefore, the total fuel consumption rate is:

$$\dot{m}_{f,tot,k} = \begin{cases} \dot{m}_{f,k} + \dot{m}_{f,cd,k} & \text{for } es_k = 1 \text{ or } fco_k = 1 \\ \dot{m}_{f,k} & \text{otherwise} \end{cases}$$

$$(80)$$

where $\dot{m}_{f,k}$ is interpolated from the ICE fuel rate map (see eq.28) and $\dot{m}_{f,cd,k}$ is the fuel penalty for ICE cold starts (0.1 g/s); some reference values for the energetic cost of engine start can be found in (Engbroks *et al.* 2019).

When the ICE state goes from 0 to 1, i.e., from off to on, the ICE fuel cut-off status fco_k is equal to 1, otherwise, it is set to be 0.

7. SIMULATION RESULTS

The DP formulation is used to find the global optimal solution to the energy management of the PHEV of interest during charge-sustaining operation. These simulation results are used to assess the effect of the gearshift and ICE start losses.

7.1 DP solution

Simulation results over three repetitions of the World-wide harmonized Light duty Test Cycle (WLTC) class 3, version 3.2 (Tutuianu *et al*., 2015) during charge-sustaining vehicle operation are discussed here.

The DP solution is able to comply with the final constrain imposed to the SOC since its final value is 50.01% (A 10% range around the initial SOC value of 50% is regarded as acceptable). In Fig. 10, it can be seen that the SOC almost repeats for each of the three WLTCs undertaken by the vehicle. Moreover, the optimal solution shows that keeping the SOC within a narrow range (less than 2 % in this case) around the required final value is the best way to proceed in terms of reducing the overall fuel consumption.These observations on the behavior of the optimal SOC trajectory are in agreement with the results presented in previous works (Onori *et al*., 2010).
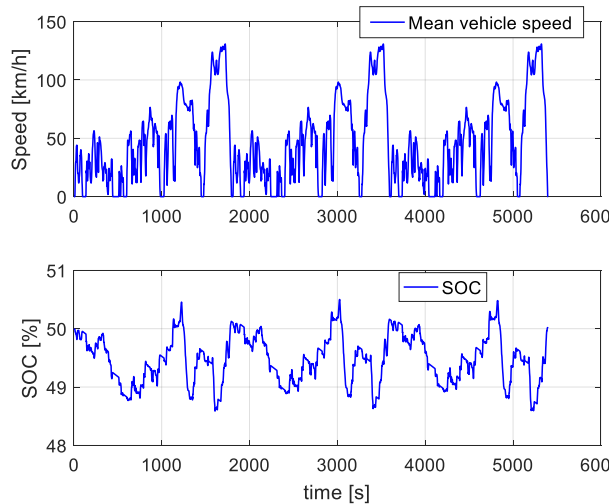

Figure 10. State of charge.

Figure 11 shows how the total torque request at the EM shaft is distributed during the last repetition of the driving schedule. An interesting observation to be made is that torque assist with the EM is used in a few occasions. The vehicle operates mostly in ICE-only mode or EV-mode. Thus, parallel hybrid mode is mainly seen in the form of the ICE power being used to recharge the battery cells. It can also be appreciated that the ICE torque is generally higher than 50 Nm, instead, lower requests are seen for the EM. Moreover, no mechanical braking is needed during the entire simulation, i.e., the electrical path powertrain components are capable of reusing all the energy needed to decelerate the vehicle.
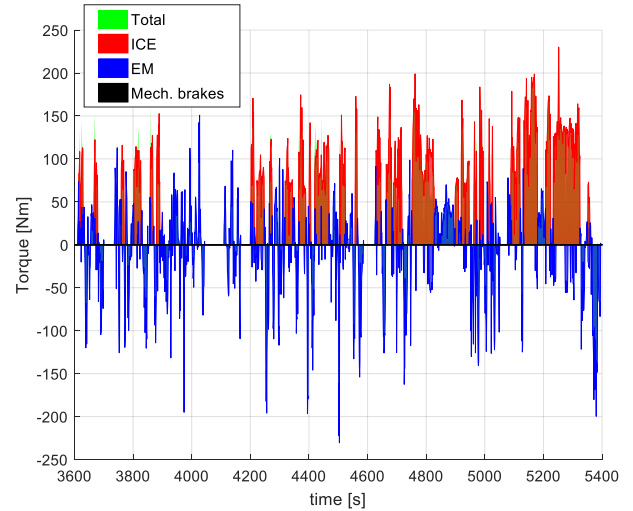

Figure 11. Torque split (3rd repetition).

The ICE operating points are shown in Fig.12. These points are concentrated in the ICE map region that corresponds to the lowest fuel consumption. This is expected considering that the arc cost defined in Eq. 63 represents the instantaneous fuel flow rate. Moreover, since the cost to be minimized depends directly on the use of the ICE, it is also reasonable for the mean efficiency of the selected operating points to be close to the maximum possible value. The mean ICE efficiency is 31.87% while the highest possible value is around 35%.

Figure 12 also illustrates the 82 ICE starts present in the results. Furthermore, it is worth mentioning that the fuel cut-off functionality is used several times during vehicle operation. Note also that the torque and speed limitations imposed are respected by the DP solution.
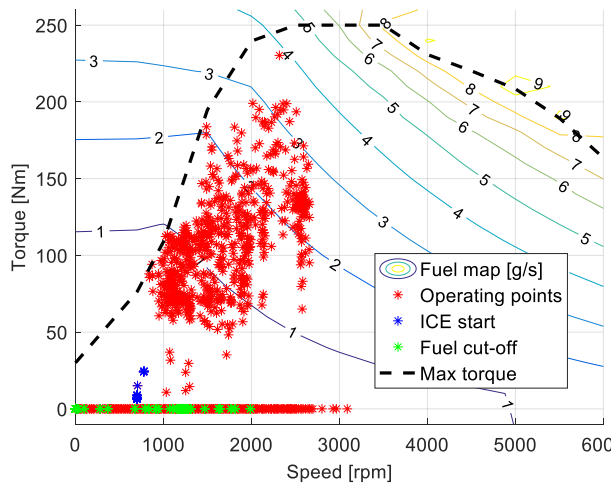
Figure 12. ICE operating points.

On the other hand, the EM operating points can be seen in Fig. 13. Note that the continuous torque limit is only breached to maximize the quantity of regenerative braking energy. The mean efficiency of the EM during the cycle is 83.32%.
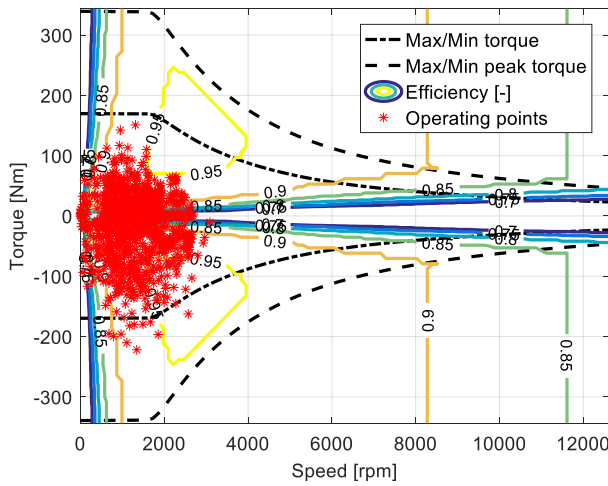

Figure 13. EM operating points.

Finally, as a result of the EMS found with the DP technique, the total fuel consumption is 2643 g, as shown in Fig. 14.
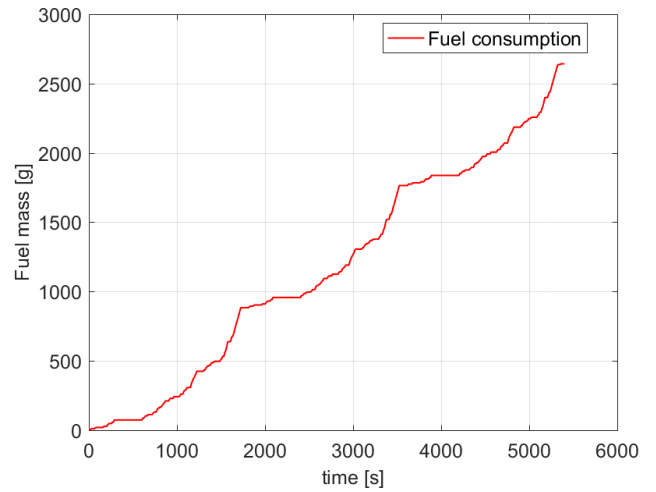

Figure 14. Fuel consumption.

7.2 Effect of the gearshift and ICE start losses

To assess the effects of the ICE start and gearshift losses in the solutions obtained, the results of a simulation of three repetitions of the cycle described in section 7.1 are compared for different cases:

- considering both ICE start and gearshift losses
- considering only the gearshift losses
- neglecting both gearshift and ICE start losses (together with the fuel penalties discussed in section 6.4).

Table 2. Effect of gearshift and ICE start losses.

	Gearshift + ICE start losses	Gearshift losses	No losses
Total number of gearshift	446	550 (+23%)	1504 (+237%)
Total number of ICE start events	82	317 (+287%)	256 (+216%)
Fuel consumption	2643	2540 (-3.4%)	2524 (-4.5%)

Table 2 shows the total number of gearshifts and ICE starts events together with the cumulative fuel consumption for all the cases considered. In parenthesis, it is reported the percentage difference with respect to the solution that accounts for both sources of dissipation.

Obviously, note that considering both types of losses, the fuel consumption becomes higher than in the other two cases.

Furthermore, according to the data presented in Tab.2, the number of gearshift maneuvers increases significantly when the associated losses are neglected. This is clearly seen in Fig.15, which also shows that, when all the losses are accounted for, the gearshift schedule does not present any gear hunting behavior. Generally speaking, when a gearshift is made, the new gear is maintained for at least 3 s.
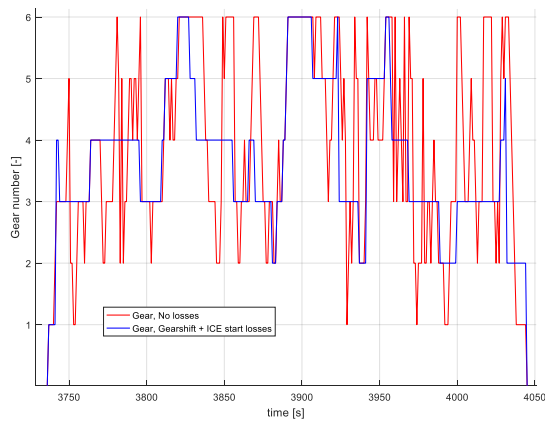

Figure 15. Gearshift schedule: Gearshift + ICE start losses vs. No losses.

Finally, Fig. 16 shows the statistics regarding the ICE state: the number of instances in which the ICE is on, disengaged and engaged but not on (fuel cut-off) for less than 5 s is reported.

Results show that a more intermittent use of the ICE is encountered when the outputs from the loss models developed for the transient events mentioned before are not integrated into the DP formulation.

In Fig. 16, it can be appreciated that, when all the losses are accounted for, the ICE is never disengaged for less than 5 s. Moreover, only in a few instances this component is on for 2 or 3 s. Instead, for the other two cases, the number of times in which the ICE is on for less than 5 s is considerably higher. For example, the ICE is on for just 1 s around 40 times for both cases. This follows from the fact that removing the ICE start losses implies that this component can be started without consuming any energy. On the other hand, the quantity of instances in which the ICE is disengaged for a short period of time also rises significantly. Note that the increase is higher for the case in which only gearshift losses are considered, impliying a relationship between the losses of these two transient events. Such connection can be understood from the results of the energy request calculation during upshift maneuvers

presented in Figure 7. During upshifts, having the quick-disconnect clutch engaged implies decelerating a higher inertia that can either help on decresing the total torque request or increase the power available for regeneration. This shows that neglecting the ICE start losses could lead to an unrealistic use of the ICE inertia to overcome gearshift losses. Furthermore, these considerations also justify the higher amount of 1 s fuel cut-offs, 90, observed when only neglecting the ICE start losses, with respect to the 13 seen when also gearshift losses are not considered.
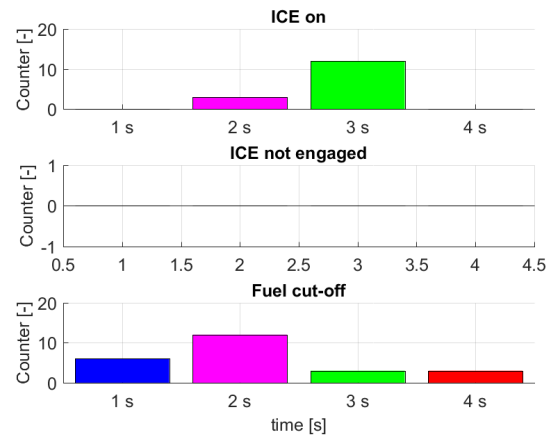
a)   Gearshift + ICE start losses
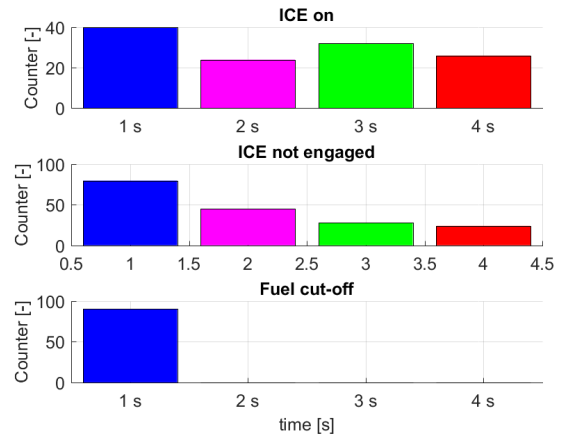
b)   Gearshift losses
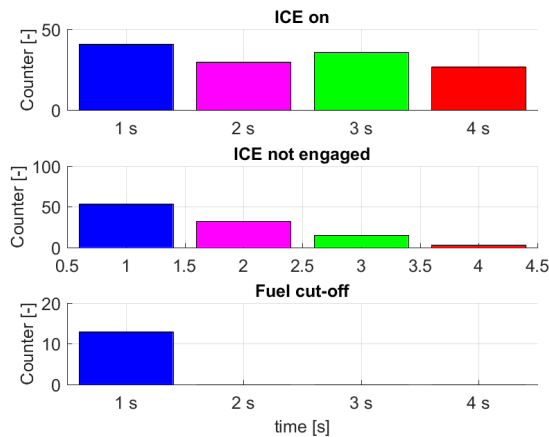
c)   No losses

Figure 16. Effect of Gearshift and ICE start losses: ICE state.

8. CONCLUSION

The electrification of powertrains equipped with DCTs offers the possibility of improving both the vehicle dynamic performance and the energy consumption. In this paper, DP is employed to find the global optimal solution to the energy management of a PHEV architecture. The general problem formulation is given. Each state and control variable is defined; moreover, the constrains imposed to state and control variables are also reported.

A backward quasi-static model of the vehicle is developed. The model is designed to properly account for the energy needed to perform gearshift and ICE start operations. This allows to develop control strategies in which these maneuvers are undertaken when it is convenient in terms of the overall energy consumption with the extra benefit of having an EMS in which transient events are not frequently requested, thus improving also the vehicle drivability.

Finally, the effects of integrating in the DP formulation the loss models developed for gearshift and ICE start events are presented. It is noted that when both sources of losses are considered, there is no gear hunting behavior in the results nor chattering in the ICE state. In addition, the analysis shows that, as expected, the number of gearshifts increases significantly when the associated losses are neglected. Another interesting conclusion is that neglecting the ICE start losses could lead to an unrealistic use of the ICE inertia to overcome the gearshift losses.

REFERENCES

Amisano F. *et al.*, (2014). Automated manual transmission with a torque gap filler part 1: Kinematic analysis and dynamic analysis, in *Proc. IMechE, Part D: Journal of Automobile Engineering.* **228**, **11**, 1247–1261.

Bellman, R.E. and Dreyfus, S.E. (2015). *Applied Dynamic Programming*. Princeton University Press.

Bertsekas, D. (1995). *Dynamic Programming and Optimal Control*. Belmont, MA: Athena Scientific.

Bianchi D, Rolando L, Serrao L, *et al.*, (2010). A rule-based strategy for a series/parallel hybrid electric vehicle: an approach based on dynamic programming, in *ASME 2010 Dynamic Systems and Control Conference*. 507–514.

Böhme, T. J. and Frank, B. (2017) *Hybrid Systems, Optimal Control and Hybrid Vehicles : Theory, Methods and Applications*, 1st ed. Cham: Springer International Publishing.

Bovee, K. M. (2015). Optimal Control of Electrified Powertrains with the Use of Drive Quality Criteria, Ohio State University.

Boyd, S. P. and Vendenberghe, L. (2004). *Convex Optimization*. New York, NY: Cambridge University Press.

Elbert, P., Nüesch, T., Ritter, A., Murgovski, N. and Guzzella, L., (2014). Engine On/Off Control for the Energy Management of a Serial Hybrid Electric Bus via Convex Optimization, *IEEE Trans. Veh. Technol.*, **63**, **8**, 3549–3559.

Engbroks, L., Knappe, P., Goerke, D., Schmiedler, S. et al., Energetic Costs of ICE Starts in (P)HEV – Experimental Evaluation and Its Influence on Optimization Based Energy Management Strategies, *SAE Technical Paper* 2019-24-0203, 2019, doi:10.4271/2019-24-0203.

Galvagno, E., Velardocchia, M. and Vigliani, A. (2011). Dynamic and kinematic model of a dual clutch transmission, *Mech. Mach. Theory*, **46**, **6**, 794–805.

Galvagno, E., Guercioni, G. R. and Vigliani, A. (2016). Sensitivity Analysis of the Design Parameters of a Dual-Clutch Transmission Focused on NVH Performance, *SAE Tech. Pap. 2016-01-1127*.

Galvagno, E., Velardocchia, M. and Vigliani, A. (2018). Transient response and frequency domain analysis of an electrically variable transmission. *Advances in Mechanical Engineering*, **10**, **5**, 1–12.

Gao, B., Lei, Y., Ge, A., Chen, H. and Sanada, K., (2011). Observer-based clutch disengagement control during gear shift process of automated manual transmission, *Veh. Syst. Dyn.*, **49**, **5**, 685–701.

Guercioni, G.R. and Vigliani, A. (2019). Gearshift control strategies for hybrid electric vehicles: a comparison of powertrains equipped with automated manual transmissions and dual-clutch transmissions. *Proc. IMechE, Part D: Journal of Automobile Engineering*, **233**, **11**, 2761–2779.

Guiggiani, M. (2014). *The science of vehicle dynamics: handling, braking, and ride of road and race cars*, 1st ed. Springer Netherlands.

Guzzella, L. and Amstutz, A. (1999). CAE tools for quasi-static modeling and optimization of hybrid powertrains, *IEEE Trans. Veh. Technol.*, **48**, **6**, 1762–1769.

Guzzella, L. and Sciarretta, A. (2013). *Vehicle Propulsion Systems: Introduction to Modeling and Optimization*, 3rd ed. Springer-Verlag Berlin Heidelberg.

Johannesson, L., Asbogard, M. and Egardt, B. (2007). Assessing the Potential of Predictive Control for Hybrid Vehicle Powertrains Using Stochastic Dynamic Programming, *IEEE Trans. Intell. Transp. Syst.*, **8**, **1**, 71–83.

Khodabakhshian, M., Feng, L. and Wikander, J. (2013). Optimization of Gear Shifting and Torque Split for Improved Fuel Efficiency and Drivability of HEVs, *SAE Tech. Pap. 2013-01-1461*.

Kim, N., Cha, S. and Peng, H. (2011). Optimal Control of Hybrid Electric Vehicles Based on Pontryagin's Minimum Principle, *IEEE Trans. Control Syst. Technol.*, **19**, **5**, 1279–1287.

Kim, N. and Rousseau, A. (2012). Sufficient conditions of optimal control based on Pontryagin's minimum principle for use in hybrid electric vehicles, *Proc. Inst. Mech. Eng. Part D J. Automob. Eng.*, **226**, **9**, 1160–1170.

Kirk, D. E. (1998). *Optimal Control Theory - An Introduction*. Dover Publications.

Lin, C.C., Peng, H,. Grizzle, J.W. and Kang, J.M. (2003). Power management strategy for a parallel hybrid electric truck, *IEEE Trans. Control Syst. Technol.*, **11**, **6**, 839–849.

Lin, C.C., Filipi, Z., Louca, L., Peng, H., Assanis, D. and Stein, J. (2004). Modelling and control of a medium-duty hybrid electric truck, *Int. J. Heavy Veh. Syst.*, **11**, **3–4**, 349–371.

Ngo, V. D., Hofman, T., Steinbuch, M. and Serrarens, A. (2012a). Effect of gear shift and engine start losses on control strategies for hybrid electric vehicles, in *26th Electric Vehicle Symposium 2012*, **5**, 125–136.

Ngo, V. D., Hofman, T., Steinbuch, M. and Serrarens, A. (2012b). Optimal Control of the Gearshift Command for Hybrid Electric Vehicles, *IEEE Trans. Veh. Technol.*, **61**, **8**, 3531–3543.

Ngo, V. D., Navarrete, J. A. C., Hofman, T., Steinbuch, M. and Serrarens, A. (2013). Optimal gear shift strategies for fuel economy and driveability, *Proc. Inst. Mech. Eng. Part D J. Automob. Eng.*, **227**, **10**, 1398–1413.

Onori, S., Serrao, L. and Rizzoni, G. (2010). Adaptive Equivalent Consumption Minimization Strategy for Hybrid Electric Vehicles, in *ASME 2010 Dynamic Systems and Control Conference*, 499–505.

Onori, S., Serrao, L. and Rizzoni, G. (2016) *Hybrid Electric Vehicles: Energy Management Strategies*, 1st ed. Springer-Verlag London.

Onori, S. and Tribioli, L. (2015). Adaptive Pontryagin's Minimum Principle supervisory controller design for the plug-in hybrid GM Chevrolet Volt, *Appl. Energy*,. **147**, 224–234.

Opila, D. F., Wang, X., McGee, R., Cook, J. A. and Grizzle, J. W. (2009). Performance comparison of hybrid vehicle energy management controllers on real-world drive cycle data, in *2009 American Control Conference*, 4618–4625.

Opila, D. F., Wang, X., McGee, R., Gillespie, R. B., Cook, J. A. and Grizzle, J. W. (2012a). An Energy Management Controller to Optimally Trade Off Fuel Economy and Drivability for Hybrid Vehicles, *IEEE Trans. Control Syst. Technol.*, **20**, **6**, 1490–1505.

Opila, D. F., Wang, X., McGee, R., and Grizzle J. W., (2012b). Real-Time Implementation and Hardware Testing of a Hybrid Vehicle Energy Management Controller Based on Stochastic Dynamic Programming," *J. Dyn. Syst. Meas. Control*, **135**, **2**, pp. 21002-21002–11.

Ostertag, E. (2011). *Mono- and Multivariable Control and Estimation: Linear, Quadratic and LMI Methods*, 1st ed. Springer-Verlag Berlin Heidelberg.

Piccolo, A., Ippolito, L., Galdi, V. and Vaccaro, A. (2001) Optimisation of energy flow management in hybrid electric vehicles via genetic algorithms, in *2001 IEEE/ASME International Conference on Advanced Intelligent Mechatronics. Proceedings (Cat. No.01TH8556)*, **1**, 434–439.

Rizzoni, G., Guzzella, L. and Baumann, B. M. (1999). Unified modeling of hybrid electric vehicle drivetrains, *IEEE/ASME Trans. Mechatronics*, **4**, **3**, 246–257.

Salmasi, F. R. (2007). Control Strategies for Hybrid Electric Vehicles: Evolution, Classification, Comparison, and Future Trends, *IEEE Trans. Veh. Technol.*, **56**, **5**, 2393–2404.

Serrao, L., Onori, S.and Rizzoni, G. (2011). A Comparative Analysis of Energy Management Strategies for Hybrid Electric Vehicles, *ASME J. Dyn. Syst. Meas. Control*, **133**, **3**, 31012.

Sciarretta, A., Back, M. and Guzzella, L. (2004). Optimal control of parallel hybrid electric vehicles, *IEEE Trans. Control Syst. Technol.*, **12**, **3**, 352–363.

Sundström O. and Guzzella, L. (2009). A generic dynamic programming Matlab function, in *2009 IEEE International Conference on Control Applications*, 1625–1630.

Tutuianu M. *et al.*, (2015). Development of the World-wide harmonized Light duty Test Cycle (WLTC) and a possible pathway for its introduction in the European legislation, *Transp. Res. Part D Transp. Environ.*, **40**, 61–75.

Waschl, H., Kolmanovsky, I., Steinbuch, M. and del Re, L. (2014). *Optimization and Optimal Control in Automotive Systems*, 1st ed., vol. 455. Springer International Publishing.